

High-magnetic field characterization of magnetocaloric effect in FeZrB(Cu) amorphous ribbons

P. Alvarez-Alonso, J. L. Sánchez Llamazares, C. F. Sánchez-Valdés, M. L. Fdez-Gubieda, Pedro Gorria, and J. A. Blanco

Citation: *Journal of Applied Physics* **117**, 17A710 (2015); doi: 10.1063/1.4907188

View online: <http://dx.doi.org/10.1063/1.4907188>

View Table of Contents: <http://scitation.aip.org/content/aip/journal/jap/117/17?ver=pdfcov>

Published by the [AIP Publishing](#)

Articles you may be interested in

[Magnetocaloric effect in Fe-Zr-B-M \(M=Ni, Co, Al, and Ti\) amorphous alloys](#)

J. Appl. Phys. **116**, 093910 (2014); 10.1063/1.4895048

[Enhanced refrigerant capacity and magnetic entropy flattening using a two-amorphous FeZrB\(Cu\) composite](#)

Appl. Phys. Lett. **99**, 232501 (2011); 10.1063/1.3665941

[Amorphous-FeCoCrZrB ferromagnets for use as high-temperature magnetic refrigerants](#)

J. Appl. Phys. **99**, 08K909 (2006); 10.1063/1.2172234

[Characterization of amorphous FeZrB\(Cu\) alloys by the inductance spectroscopy method](#)

J. Appl. Phys. **87**, 7112 (2000); 10.1063/1.372947

[Effects of Co addition on magnetic properties and nanocrystallization in amorphous Fe₈₄Zr_{3.5}Nb_{3.5}B₈Cu₁ alloy](#)

J. Appl. Phys. **86**, 6301 (1999); 10.1063/1.371690

The advertisement features a blue background with a glowing light effect on the right side. On the left, there is a small image of the 'AIP Applied Physics Reviews' journal cover, which shows a 3D grid structure. The main text 'NEW Special Topic Sections' is written in large, white, sans-serif font. Below this, the text 'NOW ONLINE' is in yellow, followed by 'Lithium Niobate Properties and Applications: Reviews of Emerging Trends' in white. The AIP Applied Physics Reviews logo is in the bottom right corner.

NEW Special Topic Sections

NOW ONLINE
Lithium Niobate Properties and Applications:
Reviews of Emerging Trends

AIP Applied Physics
Reviews

High-magnetic field characterization of magnetocaloric effect in FeZrB(Cu) amorphous ribbons

P. Alvarez-Alonso,^{1,a)} J. L. Sánchez Llamazares,² C. F. Sánchez-Valdés,²
 M. L. Fdez-Gubieda,^{1,3} Pedro Gorria,⁴ and J. A. Blanco⁵

¹Departamento de Electricidad y Electrónica, Universidad del País Vasco (UPV/EHU), 48940 Leioa, Spain

²Instituto Potosino de Investigación Científica y Tecnológica A.C., Camino a la Presa San José 2055 Col.

Lomas 4^a, San Luis Potosí, S.L.P. 78216, Mexico

³BCMaterials, Edificio 500, Parque Científico y Tecnológico de Zamudio, 48160 Derio, Spain

⁴Departamento de Física & IUTA, EPI, Universidad de Oviedo, 33203 Gijón, Spain

⁵Departamento de Física, Universidad de Oviedo, Calvo Sotelo st. s/n, 33007 Oviedo, Spain

(Presented 6 November 2014; received 22 September 2014; accepted 16 October 2014; published online 6 February 2015)

The magnetic and magnetocaloric properties of a series of Fe-rich FeZrB(Cu) amorphous ribbons were investigated under magnetic field values up to $\mu_0 H$ of 8 T. A correlation between the saturation magnetization and the maximum magnetic entropy change $|\Delta S_M^{\text{peak}}|$ is clearly evidenced. Although these metallic glasses show relatively low $|\Delta S_M^{\text{peak}}|$ values (from 3.6 to 4.4 J kg⁻¹ K⁻¹ for $\mu_0 \Delta H = 8$ T), the $\Delta S_M(T)$ curve broadens upon the increase in $\mu_0 \Delta H$, giving rise to a large refrigerant capacity RC (above 900 J kg⁻¹ for $\mu_0 \Delta H = 8$ T). Using the universal curve method for rescaling the $\Delta S_M(T, \mu_0 \Delta H)$ curves, we found a collapse of the curves around the Curie temperature. However, in the low-temperature range the curves do not match into a single one due to the existence of magnetic frustration. © 2015 AIP Publishing LLC.

[<http://dx.doi.org/10.1063/1.4907188>]

INTRODUCTION

Fe-rich FeZrB(Cu) metallic glasses display striking magnetic behaviors such as low-temperature magnetic frustration and magneto-volume anomalies below the Curie temperature, T_C , due to the strong competition between Fe-Fe magnetic interactions.¹⁻⁴ Furthermore, the value of T_C scales almost linearly with the Fe content in the 210–350 K range,^{4,5} and can be easily selected by changing the composition. The latter is of particular interest in magnetocaloric (MC) materials for: (a) developing active magnetic regenerators operating around room temperature⁶ and (b) designing two-phase MC composites with a table-like shape of the $\Delta S_M(T)$ curve. This usually improves the refrigerant capacity, RC ,^{7,8} an important figure of merit that measures the transferable heat in an ideal thermodynamic cycle from the cold to the hot reservoirs at temperatures T_{cold} and T_{hot} , respectively.^{9,10}

However, for these purposes, the materials must fulfill other requirements: to exhibit analogous values for the maximum magnetic entropy change, $|\Delta S_M^{\text{peak}}|$, and also similar shaped $\Delta S_M(T)$ curves. Previous studies reported that for $\mu_0 \Delta H \leq 5$ T, the FeZrBCu ribbons satisfy both conditions.¹¹ Moreover, the similarity of their $\Delta S_M(T)$ curves was verified in the framework of the so-called “universal curve.”¹¹ In this way, it was shown theoretically, and verified phenomenologically for $\mu_0 \Delta H$ up to 5 T, that the $\Delta S_M(T, \mu_0 \Delta H)$ curves of different materials with similar critical exponents collapse into a single curve when properly rescaled.¹²⁻¹⁴ The so-

called “universal curve” serves to extrapolate the magnetic entropy change to higher $\mu_0 \Delta H$ values and wider temperature ranges,¹⁵ and to reveal the presence of magnetic inhomogeneities.¹¹

In this study, we investigate the magnetic and magnetocaloric properties of several Fe-rich FeZrB(Cu) amorphous ribbons and test the validity of the phenomenological universal curve up to high values of the magnetic field change $\mu_0 \Delta H$ of 8 T.

EXPERIMENTAL PROCEDURE

Seven amorphous ribbons with chemical composition given by: Fe₉₀Zr₁₀, Fe₉₀Zr₉B₁, Fe₉₁Zr₇B₂, Fe₉₀Zr₈B₂, Fe₈₈Zr₈B₄, Fe₈₆Zr₇B₆Cu₁, and Fe₈₇Zr₆B₆Cu₁ were fabricated by melt spinning from arc melted bulk alloys. The amorphous character of the samples was confirmed by X-ray diffraction (no traces of crystalline phases were detected).

Magnetization measurements were performed on a Quantum Design PPMS-9T platform by using the vibrating sample magnetometer option. The T_C of samples was determined from the temperature dependence of the magnetization, $M(T)$, measured under a low applied magnetic field $\mu_0 H$ of 5 mT. The isothermal magnetization curves, $M(\mu_0 H)$, were measured up to $\mu_0 H = 8$ T from 50 to 400 K with T -steps of 10 K. The $\Delta S_M(T)$ curve for each sample was obtained by numerical integration of the Maxwell relation (i.e., $\Delta S_M(T, \mu_0 H) = \mu_0 \int_0^{\mu_0 H} \left(\frac{\partial M(T', \mu_0 H')}{\partial T'} \right)_{T'=T} dH'$).⁶

For a given value of the magnetic field change $\mu_0 \Delta H$, RC can be estimated on a first approach as the product $|\Delta S_M^{\text{peak}}| \times \delta T_{\text{FWHM}}$.¹⁰ In this definition, δT_{FWHM}

^{a)}Author to whom correspondence should be addressed. Electronic mail: pablo.alvarez@ehu.es.

corresponds to the full-width at half-maximum of the $\Delta S_M(T)$ curve [i.e., $\delta T_{FWHM}(\mu_0\Delta H) = T_{hot} - T_{cold}$, with T_{hot} and T_{cold} the working temperature ends of the refrigerant thermodynamic cycle].

The phenomenological universal curve was obtained by an appropriate renormalization of the $\Delta S_M(T)$ curves determined for the various $\mu_0\Delta H$ values. The procedure for each $\mu_0\Delta H$ value is:¹⁶ (a) the $\Delta S_M(T)$ curves are normalized to $|\Delta S_M^{peak}|$; (b) the temperature axis is rescaled below and above T_C by imposing two temperatures, Tr_1 and Tr_2 , related to two reference points at each side of the $\Delta S_M(T)$ curve that corresponds to a certain fraction of $|\Delta S_M^{peak}|$ (i.e., $a \times |\Delta S_M^{peak}|$), with a an arbitrary value between 0 and 1)

$$\begin{aligned} \theta &= -(T - T_C)/(Tr_1 - T_C) & T < T_C, \\ \theta &= (T - T_C)/(Tr_2 - T_C) & T > T_C. \end{aligned} \quad (1)$$

It must be pointed out that these reference temperatures do not have a physical meaning due to the arbitrariness of a . However, a is generally chosen equal to 0.5 since it corresponds to the half maximum and, therefore, Tr_1 and Tr_2 correspond to T_{cold} and T_{hot} , respectively.

RESULTS AND DISCUSSION

Fig. 1(a) shows the typical low-field $M(T)$ curves measured on heating after a zero-field-cooling procedure. All the samples exhibit a broad second-order magnetic phase transition. The value of T_C was estimated from the minimum of the $dM/dT(T)$ curve. As listed in Table I, T_C values range between 210 and 320 K. Fig. 1(c) depicts the curves at 50 K normalized to their respective value at $\mu_0H = 8$ T. The magnetic anisotropy increases with the Fe-content; in fact, for Fe at. % > 88, the ribbons hardly reach the saturation state at 8 T. Such behavior arises from the magneto-volume instabilities of these metallic glasses.^{1,2} We have estimated the saturation magnetization, M_S , of the ribbons by fitting the corresponding isothermal $M(\mu_0H)$ curve [a typical set of these $M(\mu_0H)$ curves is given in Fig. 1(b) for $Fe_{91}Zr_7B_2$] using an approach-to-saturation law.¹⁷ The temperature dependence of M_S (see inset in Fig. 1) shows that the higher the Fe content, the more pronounced the decrease of the $M_S(T)$ curves and the lower the saturation magnetization.

The samples exhibit broad $|\Delta S_M(T)|$ curves [see Fig. 2(a)] and moderate peak values for the magnetic entropy change, $|\Delta S_M^{peak}|$, in consonance with the wide magnetic phase transition observed in the $M(T)$ curves [see Fig. 1(a)]. It is also worth noting that the temperature corresponding to $|\Delta S_M^{peak}|$, T^{peak} , as well as the value of $|\Delta S_M^{peak}|$ follows a linear dependence with the at. % of Fe [see Fig. 2(b)], likewise T_C (see Table I & Refs. 4 and 5). In Fig. 2(c), we show the $|\Delta S_M^{peak}|$ vs. the saturation magnetization estimated at 50 K ($M_{S,50}$) for $\mu_0\Delta H = 2, 5$, and 8 T. A linear correlation between both magnitudes (with a positive slope increasing from 0.012 up to 0.024 when $\mu_0\Delta H$ increases from 2 to 8 T) is clearly evidenced. The highest $|\Delta S_M^{peak}|$ value corresponds to the alloy with the largest $M_{S,50}$ value (i.e., $M_{S,50} = 136 \text{ A}^2 \text{ kg}^{-1}$ for $Fe_{88}Zr_7B_6Cu_1$). A similar $|\Delta S_M^{peak}|$ vs. M_S relationship has been observed in other amorphous systems.^{18,19} Owing to

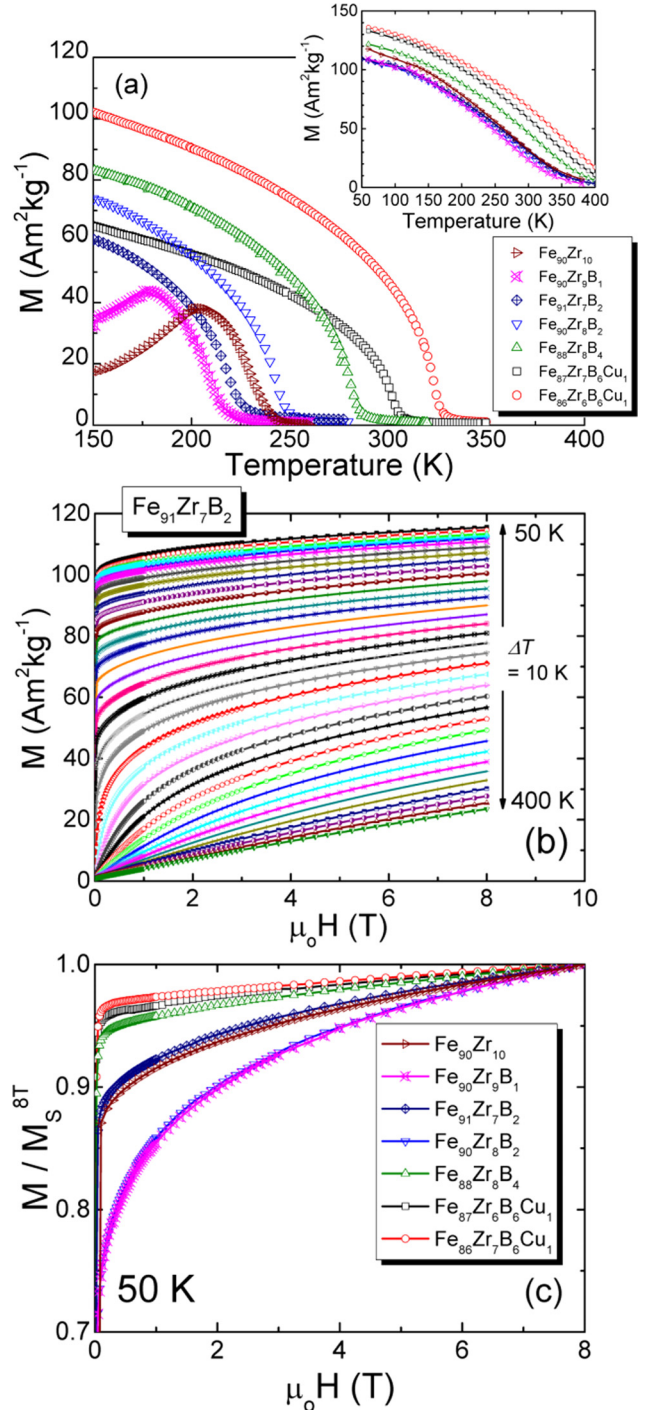
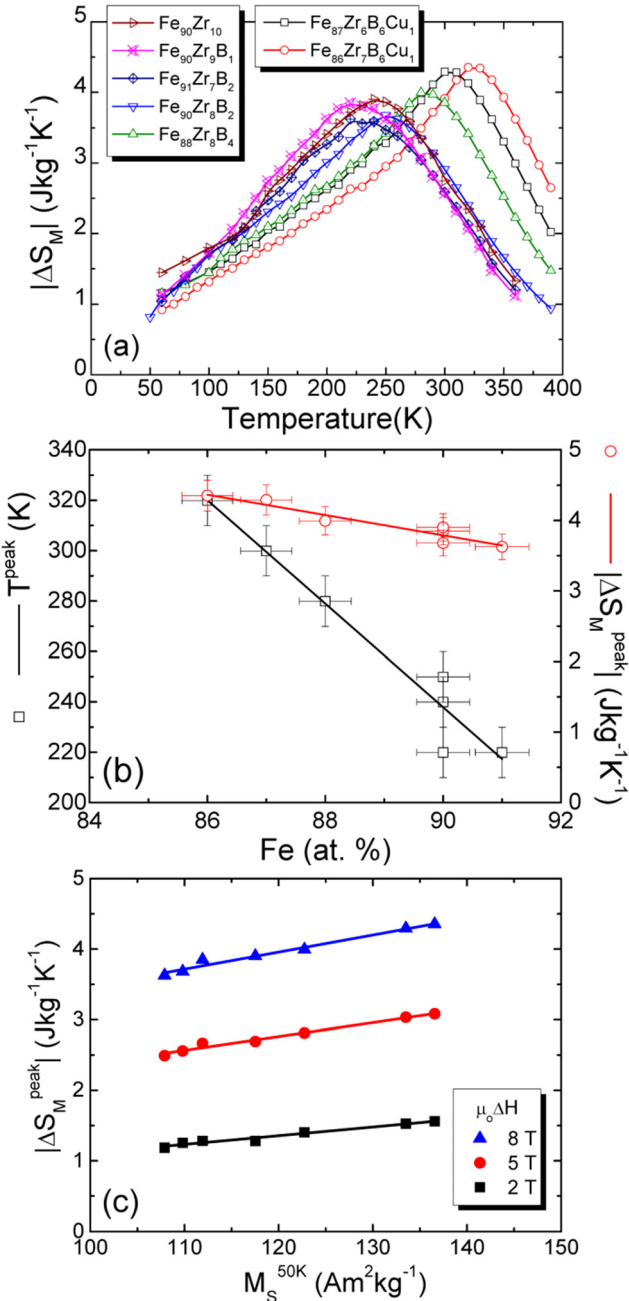
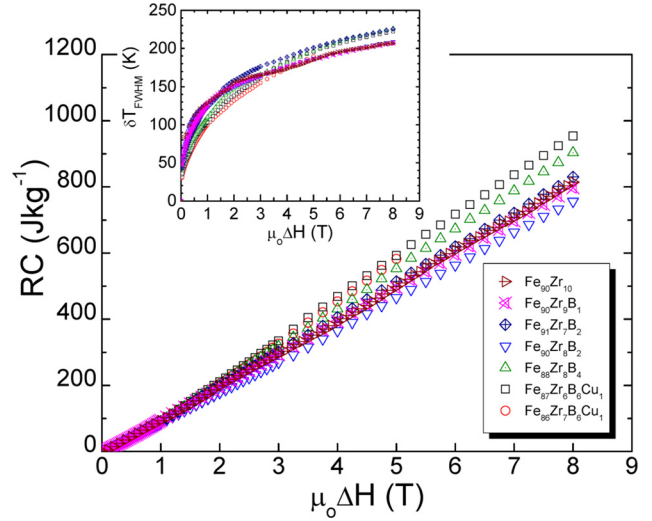


FIG. 1. $M(T)$ curves measured under $\mu_0H = 5 \text{ mT}$ (a), and $M_S(T)$ curves obtained from the fitting of the $M(\mu_0H)$ curves to the approach-to-saturation law (inset). (b) Set of $M(\mu_0H)$ measured from 50 to 400 K for the $Fe_{91}Zr_7B_2$ alloy. (c) $M(\mu_0H)$ curves at 50 K normalized to the value at $\mu_0H = 8 \text{ T}$.

their inferior M_S values and a broader ferro-to-paramagnetic phase transition, these FeZrB(Cu) amorphous alloys exhibit a lower $|\Delta S_M^{peak}|$ than that of pure Gd.²⁰ However, as shown in the inset of Fig. 3, the δT_{FWHM} values of these alloys for $\mu_0\Delta H = 5 \text{ T}$ exceed 180 K [and continuously rises as $\mu_0\Delta H$ does, because T_{cold} and T_{hot} go to lower and higher values, respectively], i.e., more than twice the working temperature span reported for Gd ($\delta T_{FWHM} \sim 70 \text{ K}$ at 5 T).²⁰ These huge width of the $|\Delta S_M(T)|$ curves explain why the RC values

TABLE I. $|\Delta S_M^{peak}|$, δT_{FWHM} , and RC for $\mu_0\Delta H = 2, 5$, and 8 T for the studied amorphous alloys.

Sample	T_C (K)	$ \Delta S_M^{peak} $ (J kg ⁻¹ K ⁻¹)			δT_{FWHM} (K)			RC (J kg ⁻¹)		
		2T	5T	8T	2T	5T	8T	2T	5T	8T
Fe ₉₀ Zr ₁₀	230 (5)	1.3	2.7	3.9	154	196	229	194	497	801
Fe ₉₀ Zr ₉ B ₁	210 (5)	1.3	2.7	3.8	153	190	215	198	492	795
Fe ₉₁ Zr ₇ B ₂	215 (5)	1.2	2.5	3.6	150	190	216	177	462	755
Fe ₉₀ Zr ₈ B ₂	240 (5)	1.3	2.6	3.7	158	201	225	198	514	830
Fe ₈₈ Zr ₈ B ₄	280 (5)	1.3	2.8	4.0	154	198	226	201	551	905
Fe ₈₇ Zr ₆ B ₆ Cu ₁	300 (5)	1.6	3.0	4.3	143	197	226	208	590	953
Fe ₈₆ Zr ₇ B ₆ Cu ₁	320 (5)	1.6	3.1	4.4	139	193	...	205	582	...

FIG. 2. (a) $\Delta S_M(T)$ curves for a magnetic field change $\mu_0\Delta H$ of 8 T. (b) $|\Delta S_M^{peak}|$ and T^{peak} as a function of the Fe at. % for an applied magnetic field change $\mu_0\Delta H = 8$ T. (c) $|\Delta S_M^{peak}|$ vs. M_S at 50 K for $\mu_0\Delta H = 2, 5$, and 8 T. Lines are guides for the eyes.FIG. 3. Applied magnetic field change dependence of the refrigerant capacity, RC. Inset: δT_{FWHM} as a function of $\mu_0\Delta H$.

reach ca. 90% that for pure Gd (Ref. 20) [see Fig. 3 and Table I for the RC values under a magnetic field change of 2, 5, and 8 T].

The degree of asymmetry exhibited by the $|\Delta S_M(T)|$ curves [see Fig. 2(a)] can be measured through the applied magnetic field dependence of $(T_{hot} - T^{peak}) - (T^{peak} - T_{cold})$ [see inset in Fig. 4(b)]. In the case of positive values, $|\Delta S_M|$ decreases slowly for $T > T_C$, whereas the negative values indicate a less marked variation of $|\Delta S_M|$ in the magnetically ordered state ($T < T_C$). The asymmetry is positive for all the studied samples under low magnetic field changes and reaches a maximum for a value of $\mu_0\Delta H$ that depends on the alloy composition. However, only the alloys with 86 and 87 Fe at. % keep the positive values in the whole magnetic field range. As expected, the effect of these asymmetries also appears in the universal curve. Fig. 4(a) shows the rescaled $\Delta S_M/\Delta S_M(\theta)$ curves for the Fe₈₆Zr₇B₆Cu₁ amorphous alloy. In the magnetically ordered state, the $\Delta S_M/\Delta S_M(\theta)$ curves for different values of the magnetic field change do not overlap for $\theta < -1$; this behavior is present in all the studied ribbons, even for low values of the magnetic field change. These irregularities indicate the existence of magnetic anomalies at low temperatures,⁹ due to either magnetic frustration or strong magneto-volume coupling. However, the curves match for $\theta > -1$, where magnetic frustration is no longer expected, thus validating the existence of a phenomenological universal curve. Moreover, all the rescaled $\Delta S_M/\Delta S_M(\theta)$ curves for $\mu_0\Delta H = 8$ T collapse in the normalized temperature range corresponding to the full width at half maximum (T_{cold} corresponds with $\theta = -1$ and T_{hot} with $\theta = 1$) and for higher temperatures, [see Fig. 4(b)], thus indicating a similar mechanism of the ferro-to-paramagnetic transition for the studied ribbons.

SUMMARY AND CONCLUSIONS

We have studied the magnetic and MC properties of a set of FeZrB(Cu) amorphous alloys under applied magnetic field values up to $\mu_0H = 8$ T. The saturation magnetization

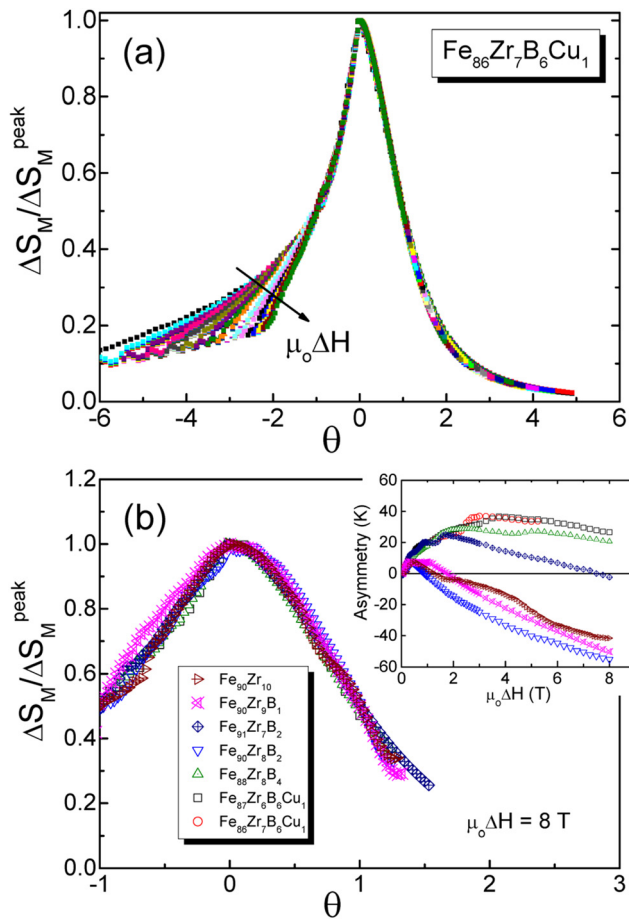


FIG. 4. (a) Rescaled $\Delta S_M(\theta)$ curve of the $\text{Fe}_{86}\text{Zr}_7\text{B}_6\text{Cu}_1$ ribbon (see text for details). (b) Comparison of the FeZrBCu alloys universal curves for $\mu_0\Delta H = 8$ T in a rescaled temperature range. Inset: Magnetic field dependence of the asymmetry of the $\Delta S_M(T)$ curves, defined as the difference $(T_{\text{hot}} - T_{\text{peak}}) - (T_{\text{peak}} - T_{\text{cold}})$.

and the temperature of the maximum of the magnetic entropy change decrease linearly with the increase of Fe-content. Although the maximum values for the magnetic entropy change are rather low (between 3.6 and $4.4 \text{ J kg}^{-1} \text{ K}^{-1}$ for $\mu_0\Delta H = 8$ T), the broad $|\Delta S_M(T)|$ curves give rise to large $RC(\mu_0\Delta H)$ values (ca. 90% of pure gadolinium at $\mu_0\Delta H = 5$ T). We also tested the validity of the phenomenological universal curve under high-applied magnetic field values: when using two reference points, the curves overlap at rescaled temperatures $\theta > -1$, but the existence of magnetic frustration avoids the collapse in the low temperature

range. Nevertheless, the universal curves of all the samples overlap for $\theta > -1$, thus suggesting a similar magnetic behavior in the ferro-to-paramagnetic transition for these Fe-rich FeZr-based amorphous ribbons.

ACKNOWLEDGMENTS

This work has been financially supported by: (a) projects CB-2010-01-156932 (CONACyT, Mexico), MAT2011-27573-C04 (MINECO, Spain), and IT711-13 (Basque Government, Spain); (b) Laboratorio Nacional de Investigaciones en Nanociencias y Nanotecnología (LINAN, IPICYT). C. F. Sánchez-Valdés thanks LINAN, IPICYT, and CONACyT (Project No. CB-2012-01-183770) for supporting his postdoctoral stay.

- ¹S. N. Kaul, V. Siruguri, and G. Chandra, *Phys. Rev. B* **45**, 12343 (1992).
- ²J. M. Barandiarán, P. Gorria, I. Orue, M. L. Fdez-Gubieda, F. Plazaola, and A. Hernando, *Phys. Rev. B* **54**, 3026 (1996).
- ³R. G. Calderón, L. F. Barquín, S. N. Kaul, J. C. Gómez Sal, P. Gorria, J. S. Pedersen, and R. K. Heenan, *Phys. Rev. B* **71**, 134413 (2005).
- ⁴J. M. Barandiarán, P. Gorria, I. Orue, M. L. Fdez-Gubieda, F. Plazaola, J. C. Gómez Sal, L. F. Barquín, and L. Fournes, *J. Phys.: Condens. Matter* **9**, 5671 (1997).
- ⁵P. Álvarez, P. Gorria, J. Sánchez Marcos, L. Fernández Barquín, and J. A. Blanco, *Intermetallics* **18**, 2464 (2010).
- ⁶A. M. Tishin and Y. I. Spichkin, *The Magnetocaloric Effect and its Applications* (IOP Publishing, Bristol, 2003).
- ⁷P. Álvarez, J. L. Sánchez Llamazares, P. Gorria, and J. A. Blanco, *Appl. Phys. Lett.* **99**, 232501 (2011).
- ⁸P. Alvarez, P. Gorria, J. L. Sánchez Llamazares, and J. A. Blanco, *J. Alloys Compd.* **568**, 98 (2013).
- ⁹K. A. Gschneidner, Jr., V. K. Pecharsky, and A. O. Tsokol, *Rep. Prog. Phys.* **68**, 1479 (2005).
- ¹⁰P. Gorria, J. L. Sánchez Llamazares, P. Álvarez, M. J. Pérez, J. Sánchez Marcos, and J. A. Blanco, *J. Phys. D: Appl. Phys.* **41**, 192003 (2008).
- ¹¹P. Álvarez, J. Sánchez-Marcos, P. Gorria, L. Fernández Barquín, and J. A. Blanco, *J. Alloys Compd.* **504**, S150 (2010).
- ¹²V. Franco, J. S. Blázquez, M. Millán, J. M. Borrego, C. F. Conde, and A. Conde, *J. Appl. Phys.* **101**, 09C503 (2007).
- ¹³V. Franco, A. Conde, V. Provenzano, and R. D. Shull, *J. Magn. Magn. Mater.* **322**, 218–223 (2010).
- ¹⁴V. Franco, J. M. Borrego, A. Conde, and S. Roth, *Appl. Phys. Lett.* **88**, 132509 (2006).
- ¹⁵V. Franco and A. Conde, *Int. J. Refrig.* **33**, 465 (2010).
- ¹⁶V. Franco, R. Caballero-Flores, A. Conde, Q. Y. Dong, and H. W. Zhang, *J. Magn. Magn. Mater.* **321**, 1115 (2009).
- ¹⁷B. D. Cullity and C. D. Graham, *Introduction to Magnetic Materials* (IEEE Press-Wiley, 2009).
- ¹⁸J. Y. Law, R. V. Ramanujan, and V. Franco, *J. Alloys Compd.* **508**, 14 (2010).
- ¹⁹V. Franco, C. F. Conde, J. S. Blázquez, A. Conde, P. Švec, D. Janičkovič, and L. F. Kiss, *J. Appl. Phys.* **101**, 093903 (2007).
- ²⁰J. F. Elliott, S. Legvold, and F. H. Spedding, *Phys. Rev.* **91**, 28 (1953).